Thin Solid Films 518 (2010) e5–e8

Contents lists available at ScienceDirect

Thin Solid Films

journal homepage: www.elsevier.com/locate/tsf

Enhancement of magnetization and dielectric properties of chromium-doped $BiFeO_3$ with tunable morphologies

Yi Du, Zhen Xiang Cheng, Shi Xue Dou, Mahboobeh Shahbazi, Xiao Lin Wang *

Institute for Superconducting and Electronic Materials (ISEM), University of Wollongong, Squires Way, Fairy Meadow, NSW, 2519, Australia

ARTICLE INFO

Available online 11 April 2010

Keywords:
Bismuth ferrite
Chromium doping
Dielectric
Magnetic
Tunable morphology

ABSTRACT

Multiferroic $BiFe_{1-x}Cr_xO_3$ ($x = 0.025$, 0.05, 0.075, and 0.1) is prepared by the hydrothermal method. Samples are systematically characterized by X-ray diffraction, Rietveld refinement, SEM, dielectric and magnetic measurements. It is found that the lattice parameters, the morphology and the size of the obtained particles strongly depend on the Cr doping level. The lattice parameters a and c and the Fe–O (1) bond lengths decrease, while the Fe–O (2) bond lengths increase, as x values rise from 0.025 to 0.1. The particle morphology changes from spherical shape for pure $BiFeO_3$ to octahedral shape for $x = 0.1$. The dielectric constant and the magnetization increase greatly with the increase of the Cr doping level. Both the M–T and the M–H results reveal that the Cr doping enhances the ferromagnetic state in the doped $BiFeO_3$. The possible reasons for the enhanced magnetic and dielectric properties are discussed briefly.

1. Introduction

Multiferroic materials with coexisting ferromagnetic and ferroelectric properties are attracting much attention nowadays [1,2]. As one of very few existing multiferroics, bismuth ferrite ($BiFeO_3$) with the perovskite structure is expected to be used for applications in ferroelectric nonvolatile memories and high temperature electronics due to its high polarization, high Curie temperature (~820 °C), and G-type antiferromagnetic Néel temperature (~375 °C) [3–6]. However, the incorporation of bismuth ferrite into practical devices is very challenging because the defects and non-stoichiometry cause low resistivity and hence a severe current leakage problem. Rare earth (RE) element substitution for bismuth in $BiFeO_3$ is found to be an efficient way to solve the problem [7–9]. Nevertheless, utilizing transition metal (TM) elements, including Cr, Co, and Mn, to substitute into Fe-sites in $BiFeO_3$ has also been proved to improve the ferroelectric and ferromagnetic properties [10–12]. Some new types of multiferroics, e.g. Bi_2FeCrO_6, with large polarization and magnetization are also predicted [13]. However, the majority of reports on TM doped $BiFeO_3$ are on thin films. Because of difficulty in preparing the pure phase, the reports on nano-/micro-particles are very few. Therefore, the influence of finite size on the lattice parameters and polar displacements of atoms should be expected to provide insight into the finite size effects on ferroelectricity as well as ferromagnetism.

In this work, micron-sized $BiFe_{1-x}Cr_xO_3$ particles with different doping levels ($x = 0.025$, 0.05, 0.075, and 0.1) were prepared via a hydrothermal method. The crystal structure of samples has been studied in detail by X-ray diffraction (XRD) refinement. The magnetic properties, such as magnetization dependence on temperature (M–T) and on field (M–H), have been investigated. The frequency dependence of the dielectric constant and dielectric loss at room temperature has also been measured.

2. Experimental details

The chromium-doped bismuth ferrite ($BiFe_{1-x}Cr_xO3$) samples were synthesized by the hydrothermal method. Bismuth nitrate ($Bi(NO_3)_3$, 99.5%), iron (III) nitrate ($Fe(NO_3)_3$, 99.5%), chromium oxide (Cr_2O_3, 99.5%) and potassium hydrate (KOH, 99%), obtained from Sigma-Aldrich, were used as starting materials. Bismuth nitrate and iron nitrate were dissolved in nitric acid with magnetic stirring for 30 min. After that, the chromium oxide was added into the light brown solution, with stirring maintained for 6 h at 80 °C until it was dissolved. KOH was introduced to induce a co-precipitation reaction. The brown precipitate was then transferred into an autoclave with a Teflon liner after being washed with distilled water. 14 mol/L potassium hydrate solution was added until the Teflon liner is 80% full. The autoclave was kept at 200 °C for 12 h, and then allowed to cool down to room temperature naturally. The obtained black powder was washed with distilled water and dried at 70 °C for 2 h.

Phase identification of the obtained powders was performed with a Philips X-ray diffractometer (XRD, Philips 1730), using Cu-Kα radiation at $\lambda = 1.54056$ Å. The lattice parameters and the crystal structure were refined using the Rietica package (Vision 1.7.7), based on the XRD results. The particle morphology and size were examined with a scanning electron microscope (SEM, JSM-6460A). The dielectric

---

* Corresponding author. Tel.: +61 2 42215766; fax: +61 2 42215731.
E-mail address: xiaolin@uow.edu.au (X.L. Wang).

0040-6090/$ – see front matter © 2010 Elsevier B.V. All rights reserved.
doi:10.1016/j.tsf.2010.03.118

constant and loss measurements were conducted using an impedance analyzer (HP-4191A IMPEDANCE/GAIN-PHASE Analyzer) in the frequency range from 100 Hz to 15 MHz at room temperature. The magnetic measurements were carried out using a magnetic properties measurement system (MPMS, Quantum Design MPMS-XL) over a wide temperature range from 5 K up to 350 K and a range of magnetic fields up to 3 T.

3. Results and discussions

Fig. 1 shows the XRD patterns of $BiFe_{1-x}Cr_xO_3$ with different doping levels ($x = 0$, 0.025, 0.05, 0.075, and 0.1). All the results can be indexed well by Joint Committee on Powder Diffraction Standards (JCPDS) card 20-0169. The crystal structure is rhombohedral and in space group *R3c*. No impurity phase was found in these samples, which means that all of the samples are single phase.

XRD refinement results for $BiFe_{1-x}Cr_xO_3$ samples are carried out as shown in Fig. 2. It can be seen that the XRD refinements fits well with the experimental data. The lattice parameters of samples with different doping levels are listed in the Table 1. The calculations verify that the lattice parameters are similar in samples with $x = 0$ and 0.025, however, the Fe–O (1) and Fe–O (2) bond lengths are shortened in $BiFe_{0.975}Cr_{0.025}O_3$. Although the c/a ratios are all equal to 2.49 with the different doping levels, lattice parameters *a*, *b*, and *c* decrease as the Cr doping level increases. Likewise, the Fe–O (1) bond lengths decease, while the Fe–O (2) bond lengths increase, as *x* values rise from 0.025 to 0.1. The ratios between Fe–O (1) and Fe–O (2) are also listed in the table, which shows the decreasing trend with increasing doping level. It can be deduced that the Fe–O octahedra in the $BiFe_{1-x}Cr_xO_3$ crystal structure are becoming more asymmetric (as shown in Fig. 2(b) by the distortion along the O (1)–Fe–O (2) direction in the inset), because of which the physical properties of the more heavily doped samples are expected to be different from those of the pure $BiFeO_3$ sample.

Fig. 3 shows SEM images of $BiFe_{1-x}Cr_xO_3$ ($x = 0$, 0.05, and 0.1) particles. The morphologies of those samples are strongly dependent on the Cr doping level. The pure $BiFeO_3$ particles are spheroidal, with a mean diameter of 30 μm. The surfaces of the particles are very rough. After chromium doping, the diameter of the particles is reduced. The $BiFe_{0.975}Cr_{0.05}O_3$ particles still retain their rough, sphere-like shape. As the Cr doping level increases to $x = 0.1$, the particle morphology changes to a uniform octahedral shape with a smooth surface, and the size of most particles is reduced to less than 15 μm.

Fig. 4 shows the dielectric constants (ϵ') of $BiFe_{1-x}Cr_xO_3$ as a function of frequency for five samples at room temperature, and the dielectric loss curves versus frequency. The frequency range applied was from 100 Hz to 15 MHz. The dielectric constants for all samples decrease with increasing frequency, which can be explained by a conventional dielectric relaxation process. It is found that the value of the dielectric constant is significantly increased by Cr substitution. For instance, the dielectric constant is 410 when $x = 0.0025$ at 600 Hz, nearly fourfold that of pure $BiFeO_3$. As more Cr ions substitute into Fe ion positions, the dielectric constant also increases and reaches its maximum when $x = 0.1$. The obtained dielectric constants were larger than that of the bulk sample prepared by conventional solid state reaction [14]. Similar to the dielectric constant, the dielectric loss also decreases with increasing frequency. Both the dielectric constant and the dielectric loss are very stable in the frequency range from 5 kHz to 15 MHz.

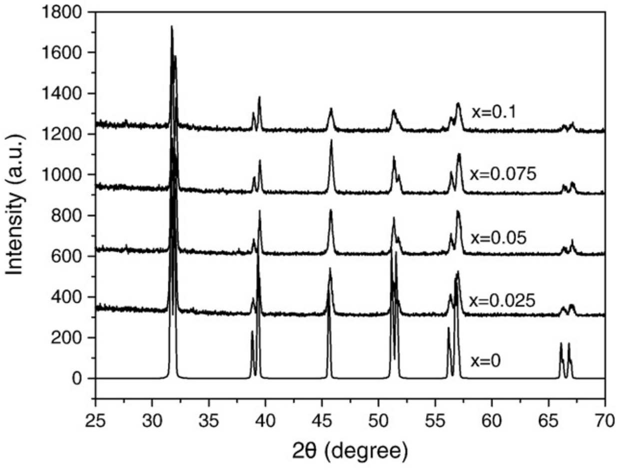

Fig. 1. XRD patterns of $BiFe_{1-x}Cr_xO_3$ ($0 \le x \le 0.1$) samples.

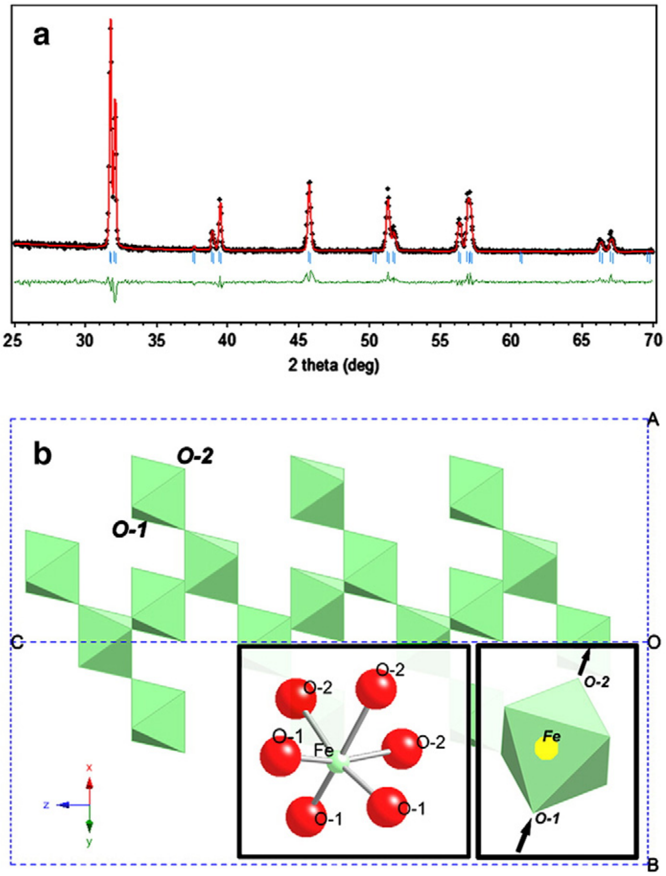

Fig. 2. XRD refinement of $BiFeO_3$ sample. (a) is the calculated result for pure $BiFeO_3$. The dashed lines are experimental data, while the solid curves are the calculation results. The vertical bars indicate the peak positions that are calculated by refinement, and the bottom solid lines indicate the differences between experimental and calculation results. (b) is a schematic diagram of the Fe–O octahedra in the $BiFe_{1-x}Cr_xO_3$ samples; the inset shows a single Fe–O octahedron with both stick–ball and polyhedron models.

The magnetic properties for $BiFe_{1-x}Cr_xO_3$ ($0 \le x \le 0.1$) samples are shown in Fig. 5. The temperature dependence of the magnetization process (zero field cooled measurement), which was measured in the temperature range from 5 K to 350 K in 2000 Oe field, indicates that all the samples have a ferromagnetic moment at room temperature, as

Table 1
Calculated lattice parameters of $BiFe_{1-x}Cr_xO_3$ ($0 \le x \le 0.1$) by refinement of XRD data.

Samples	*a* (Å)	*c* (Å)	Fe–O (1) (Å)	Fe–O (2) (Å)	(1)/(2)
$BiFeO_3$	5.58(3)	13.87(9)	1.95(9)	2.12(7)	0.921
$BiFe_{0.975}Cr_{0.025}O_3$	5.58(6)	13.88(2)	1.93(9)	2.11(9)	0.915
$BiFe_{0.95}Cr_{0.05}O_3$	5.58(2)	13.87(2)	1.93(1)	2.12(8)	0.907
$BiFe_{0.925}Cr_{0.075}O_3$	5.57(5)	13.85(9)	1.87(9)	2.15(3)	0.873
$BiFe_{0.9}Cr_{0.1}O_3$	5.57(2)	13.85(6)	1.85(6)	2.22(4)	0.834